Inductively Coupled Plasma Mass Spectrometry with an Enlarged Sampling Orifice and Offset Ion Lens. II. Polyatomic Ion Interferences and Matrix Effects

Ke Hu* and R. S. Houk

Ames Laboratory–U.S. Department of Energy, Department of Chemistry, Iowa State University, Ames, Iowa, USA

A new inductively coupled plasma mass spectrometer with an enlarged sampling orifice (1.31-mm dia.) and an offset ion lens yields very low levels of many troublesome polyatomic ions such as ArO^+, ArN^+, Ar_2^+, ClO^+, and $ArCl^+$. The signals from refractory metal oxide ions are ~1% of the corresponding metal ion signals, which is typical of most ICP-MS devices. Grounding the first electrode of the ion lens greatly reduces the severity of matrix effects to $\lesssim$ 20% loss in signal for Co^+, Y^+, or Cs^+ in the presence of 10 mM Sr, Tm, or Pb. This latter lens setting causes only a modest loss (30%) in sensitivity for analyte elements compared to the best sensitivity obtainable by biasing the first lens. Alternatively, matrix effects can also be mitigated by readjusting the voltage applied to the first lens with the matrix present. *(J Am Soc Mass Spectrom 1993, 4, 28–37)*

Although inductively coupled plasma mass spectrometry (ICP-MS) is a highly successful method for elemental and isotopic analysis, some elements still cannot be determined readily in important samples because of interferences. For example, polyatomic ions such as ArO^+, ArN^+, Ar_2^+, ClO^+, and $ArCl^+$ hamper determination of Fe, Se, V, and As. These interfering species can be attenuated somewhat by tactics such as mixed gas plasmas [1–5], removal of solvent [1, 2, 6–11], and polishing the inside of the sampling cone [12]. A high-resolution mass spectrometer [13, 14] or a collision cell [15–17] can also be used for this purpose, with the expense associated with the additional hardware necessary.

ICP-MS also suffers from matrix interferences, in which the matrix concentration affects the analyte signal. Generally, the analyte signal is suppressed as the matrix concentration increases [6, 18–21], although signal enhancements can sometimes be observed [22]. The extent of the interference depends on the plasma operating conditions and the atomic masses of both the matrix and analyte ion. Usually the interference problem is worst for a light analyte ion in the presence of a heavy matrix ion [19]. Thus, the most severe matrix interference is that of uranium matrix on lithium analyte. Gillson et al. [23] and Tanner [24] attribute the matrix interferences mainly to space charge effects that disperse the ion beam and cause loss of ions behind the skimmer and in the ion lens. Presently, this space charge effect is the most cogent explanation of the matrix interference problem.

Reasonable methods of diagnosing and compensating for interferences due to either polyatomic ions or matrix effects are available. For example, the interference of $^{40}Ar^{35}Cl^+$ on $^{75}As^+$ can sometimes be estimated by measuring the abundance of $^{40}Ar^{37}Cl^+$ and applying the appropriate isotopic correction to the total signal at m/z 75. Internal standardization is employed routinely to correct for matrix interferences [11, 25]; standard additions and isotope dilution can also be employed for this purpose. As a general rule, the compensation provided by these methods is more reliable if the extent of the interference is less severe in the first place.

The first article in this pair described the performance and characterization of a new ion lens system for ICP-MS [26]. The present article shows that this same ICP-MS device has relatively low levels of many troublesome polyatomic ions. Minor adjustments to the lens voltages also reduce the severity of matrix effects substantially. These latter results are compared with those of Ross and Hieftje [27], who found that matrix effects were greatly reduced by removing the

*Present address: Thermo Jarrell-Ash Corp., 8E Forge Parkway, Franklin, MA 02038-3148.

Address reprint requests to R. S. Houk, Ames Laboratory–U.S. Department of Energy, Department of Chemistry, Iowa State University, Ames, IA 50011.

© 1993 American Society for Mass Spectrometry
1044–0305/93/$5.00

Received March 23, 1992
Revised July 13, 1992
Accepted July 13, 1992

ion lens between the skimmer and differential pumping orifice.

Experimental

ICP-MS instrumentation. The ICP-MS device and its performance are described in the companion article [26]. Briefly, samples are introduced via a continuous flow ultrasonic nebulizer with desolvation (Model U-5000, Cetac Technologies, Omaha, NE) to an argon ICP. Ions are extracted through enlarged sampler and skimmer orifices (each 1.31-mm dia.) into an offset ion lens and quadrupole mass analyzer. Conditions particular to the present paper are noted in Table 1. Only the Channeltron detector was used.

The ion lens is shown in Figure 1. The same physical arrangement of ion lens electrodes was used throughout. Three different sets of lens voltages were evaluated. These three configurations differed mainly in the voltages applied to the first cylinder (V_1) and the cone (V_2). The lens voltages for each lens configuration (A, B, or C) are listed in Table 2. Lens A was used throughout the companion article and for the studies of background spectra in the present article. The first cylinder was biased at +3 V and the voltages applied to the other electrodes were adjusted to maximize Y^+ signal. For lens B, the first cylinder was grounded and the other voltages were readjusted to maximize Y^+ signal again. The optimum voltages for lens B were only slightly different from those for lens A. Finally, for lens C, both the first cylinder and the cone were grounded. Many of the other lenses then required substantial adjustments to the applied voltages to remaximize the ion signal.

After the optimum lens voltages were found in this manner for each configuration, the aerosol gas flow rate was readjusted to maximize Y^+ signal. As shown in Table 1, each of the three lens configurations required slightly different aerosol gas flow rates. With the load coil geometry used with this device, the plasma potential and ion kinetic energy varied somewhat with aerosol gas flow rate, which probably caused the interdependence of aerosol gas flow rate and lens voltages.

Solutions, solvents, and standards. Standards were prepared by diluting aliquots of commercial stock solutions (1000 ppm, Fisher, Fair Lawn, NJ) with distilled, deionized water (18 MΩ, Barnstead, Newton, MA). In matrix effect studies, the analyte concentration was deliberately kept rather high (1 ppm) to minimize possible contamination from impurities in the matrix elements. Blank solutions containing the matrix without analyte were analyzed; contamination was negligible. The 1% HNO_3 and 1% HCl were prepared by diluting ultrapure acids (Ultrex II, reagent grade, J. T. Baker) in distilled, deionized water. The lead matrix was so-called common lead, that is, the isotope ratios were $^{207}Pb/^{206}Pb \sim 1/1$, $^{208}Pb/^{206}Pb \sim 2/1$.

Table 1. Operating conditions*

ICP	
Forward power	1.4 kW
Aerosol gas flow rate[a]	
Lens config. A[b]	1.30 L min^{-1}
Lens config. B[b]	1.25 L min^{-1}
Lens config. C[b]	1.20 L min^{-1}
Sampling position	On center
	13 mm from downstream end of load coil
Mass Spectrometer	
Mean dc bias:	
Mass analyzer	−1.0 V
Rf-only rods	−65 V
Bias voltages on Channeltron	
Sensitivity measurements	−3000 V
Matrix effect measurements	−2700 V
Data Acquisition	
Background spectra	Multichannel scanning [11]
(Figures 2–8)	1000 sweeps
	4096 channels from *m/z* 42–85
	Dwell time 50 ms per channel
Matrix effect studies	See text
Solutions	
Matrix effect studies	1 ppm each analyte
	One matrix element per solution at 10 mM
Sensitivity measurements	0.5 ppm Co, Y
	0.2 ppm Cs
Metal oxide measurements	1 ppm Mo
	0.2 ppm La
	0.5 ppm U

* See also ref 26.
[a] These represent the aerosol gas flow rates that yield maximum Y^+ signal.
[b] See Figure 1 for diagram of lens and Table 2 for list of applied voltages.

Matrix effect studies. The analyte elements (Co, Y, and Cs) and the matrix elements (Sr, Tm, and Pb) were chosen because they are efficiently ionized in the plasma and they have significantly different atomic masses. The mass analyzer was scanned repetitively in multichannel mode through a mass window 30 mass-to-charge ratio units wide spanning each analyte peak. Thus, a separate set of scans was obtained for each analyte in each matrix. The solutions were analyzed in the following order: analyte only, analyte + matrix, analyte only. The third step (i.e., reanalysis of the solution containing only analyte) was continued until the analyte signal recovered to its original value, which took approximately 2 min. The process was repeated

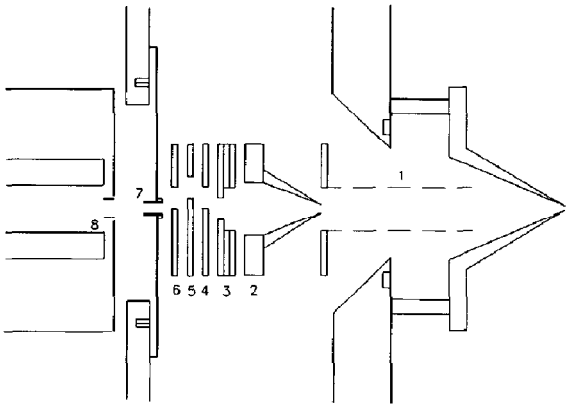

Figure 1. Ion lens configuration. The skimmer is at the far right, and the entrance rf-only rods are at the far left. The sampler is not shown. 1: perforated cylindrical electrode, 2: conical electrode, 3–6: electrodes with circular apertures, 7: differential pumping aperture, 8: ELFS entrance to rf-only rods.

6–8 times successively for each analyte in each matrix; the average matrix effects are reported below. The mass analyzer was then adjusted to the appropriate mass-to-charge window for the next analyte, and the process was repeated.

In this fashion, matrix effects were measured for each analyte in each matrix under each lens configuration (see Figure 1 and Table 2). All the results reported subsequently in Figures 9–11 were obtained successively on one day without turning the plasma off. The entire sequence of matrix effect experiments was repeated on three separate days, with consistent results.

Results and Discussion

Polyatomic Ions from Deionized Water and HNO_3 Solutions

Background spectra from m/z 42 to 85 are shown for deionized water and 1% HNO_3 in Figures 2 and 3. The lower frame in each figure is merely plotted with a more sensitive vertical scale so that weak peaks are evident. The weaker peaks appear noisy in the expanded frames because only a few counts are recorded in each channel for many of them.

Inspection of Figures 2 and 3 shows that the usual polyatomic ions are not very intense with this ICP-MS instrument. The worst one is $^{40}Ar_2^+$ at m/z 80, and it is

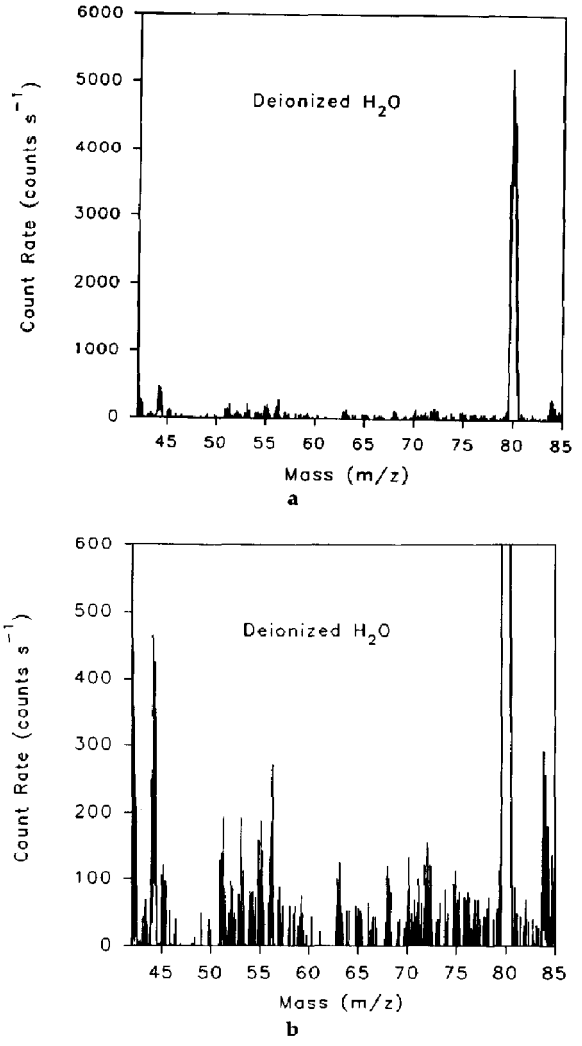

Figure 2. Background spectra obtained during nebulization of deionized distilled water for m/z 42–85.

only ~5000 counts s^{-1}. The minor isotope peaks of Ar_2^+ are not clearly distinguishable. Peaks at m/z 44 (probably CO_2^+) and m/z 84 (probably $^{84}Kr^+$) are next in abundance to Ar_2^+. From deionized water $^{40}Ar^{16}O^+$ is only ~200 counts s^{-1}. The 1% HNO_3 is a bit impure, as peaks from ClO^+ (m/z 51 and 53), $^{55}Mn^+$,

Table 2. Ion lens voltages for the various lens configurations[a]

Configuration	Ion lens voltage (V)							
	V_1	V_2	V_3	V_4	V_5	V_6	V_7	V_8
A[b]	+3	−240	−55	+2.0	−200	+14	−240	−200
B	ground	−240	−61	+3.0	−200	+13	−240	−210
C	ground	ground	−20	+28	−225	+28	−230	−230

[a] Each ion lens voltage was optimized for obtaining maximum Y^+ signals.
[b] For configurations A, B, and C, the same set of electrodes was used, as shown in Figure 1. The applied voltages were different for each configuration, as shown in this table.

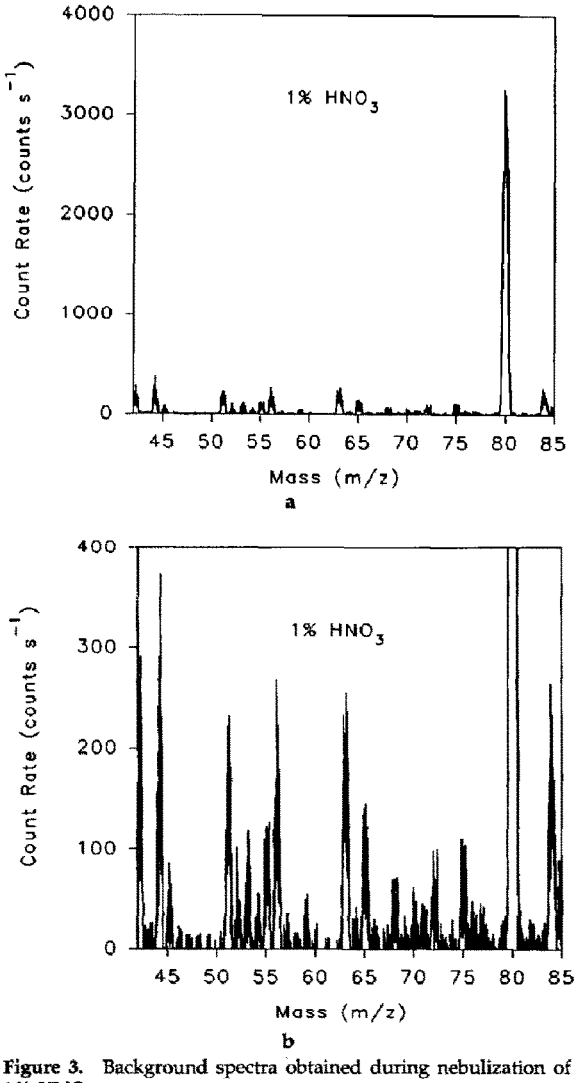

Figure 3. Background spectra obtained during nebulization of 1% HNO_3.

Cu^+ (m/z 63 and 65), and perhaps $^{75}As^+$ and/or $^{40}Ar^{35}Cl^+$ are seen. For either solvent, the absolute levels of these polyatomic ions are far below those usually seen on most other ICP-MS devices. For reference, the spectrum of Fe at 0.5 pm is shown in Figure 4. Compared to the blank spectrum (Figure 3), both $^{54}Fe^+$ and $^{56}Fe^+$ are easily seen at this level.

Polyatomic Ions from HCl and NaCl Solutions

Chlorine in any form in the sample generally leads to the troublesome polyatomic ions ClO^+ and $ArCl^+$. Background spectra from 1% HCl and 0.25% NaCl (the equivalent of 0.1% Na) are shown in Figures 5 and 6. Note that these samples are being introduced with an ultrasonic nebulizer, and the desolvation system

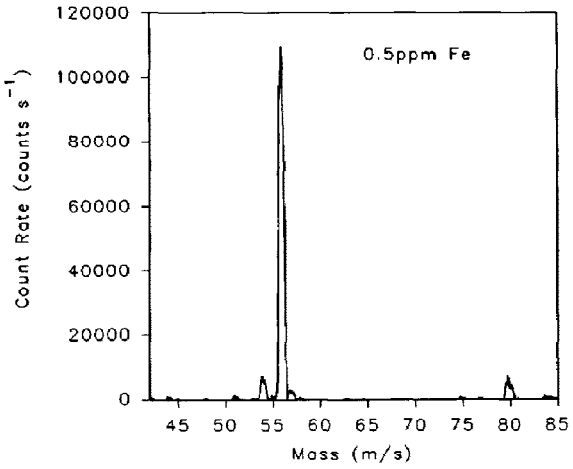

Figure 4. Mass spectrum from 0.5 ppm Fe in 1% HNO_3.

does not remove either HCl or NaCl. $ArCl^+$ is barely observable from either solution, and $^{35}Cl^{16}O^+$ is only 200–400 counts s^{-1}. The Cu^+ observed from both solutions could be from Cu impurity or possibly from Cu^+ ablated from the conical ion lens, which is made from copper. In the spectrum from 0.25% NaCl, the ratio of the peak at m/z 63 to that at m/z 65 is too high for Cu^+, so there is probably some $ArNa^+$ present at ~100 counts s^{-1}. A curious peak at m/z 62 is attributed tentatively to Na_2O^+, the sodium analog of water.

For comparison, spectra of As at 0.5 ppm in 1% HCl (Figure 7) and Cu and Co at 1 ppm in 0.25% NaCl are provided in Figures 7 and 8. In Figure 7, $^{40}Ar^{37}Cl^+$ is not distinguishable from background, even though 1% HCl is being introduced with an ultrasonic nebulizer. Some $^{40}Ar^{35}Cl^+$ (~150 counts s^{-1}) is probably evident in Figure 8. Again, these common polyatomic ions containing chlorine are observed only at quite low levels with this device.

Comparison of Polyatomic Ion Levels to Usual Values

A rigorous comparison of the levels of polyatomic ions seen in Figures 2–8 to those seen in other quadrupole ICP-MS devices is difficult for several reasons. First, many of the weak peaks shown in Figures 2–8 are probably at least partly due to metal impurities in the solvents rather than polyatomic ions. Second, polyatomic ion levels with any ICP-MS instrument are highly sensitive to operating conditions and the methods used for nebulization and solvent removal.

For these reasons, the following discussion compares polyatomic ion levels obtained recently in two papers that used an ultrasonic nebulizer with conventional desolvation, that is, heating at ~140 °C followed by condensation at ~0 °C. This nebulizer and desolvator are the same as those used in the present

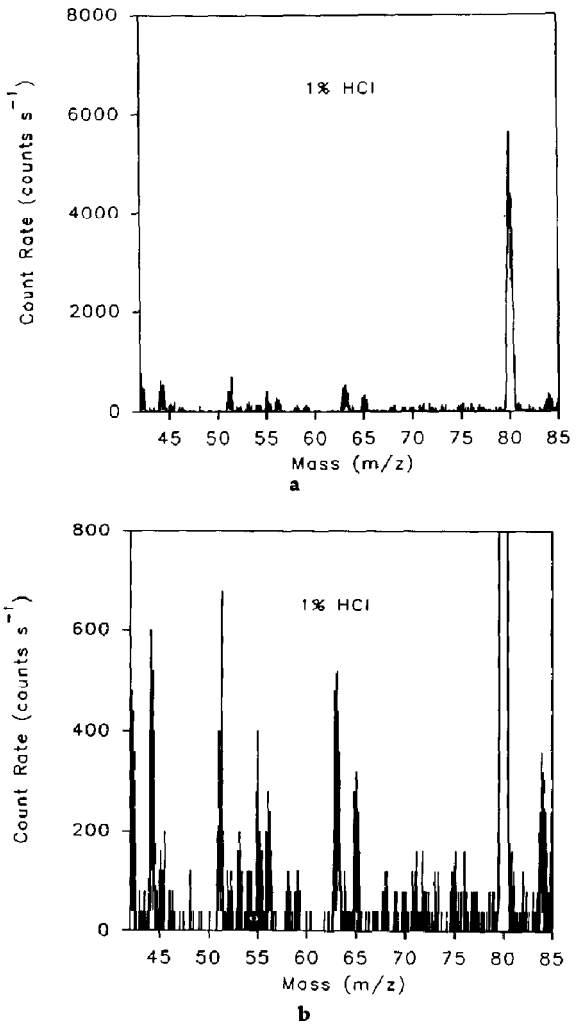

Figure 5. Background spectrum from 1% HCl.

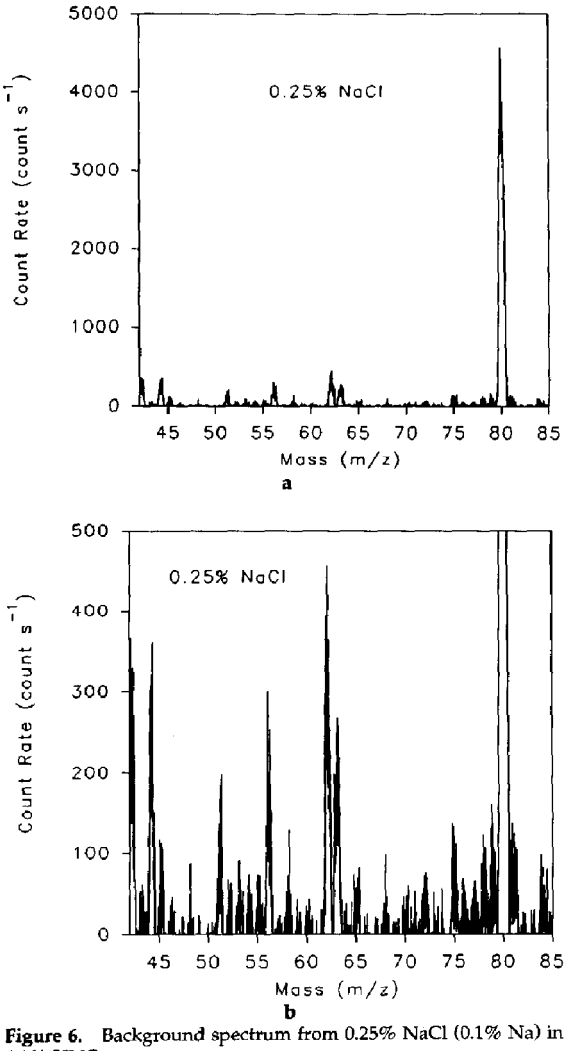

Figure 6. Background spectrum from 0.25% NaCl (0.1% Na) in 0.1% HNO_3.

work. In one paper, Xe is added to attenuate polyatomic ions [5]. In the other paper, cryogenic desolvation is employed for the same purpose [9]. In either case, the count rates and background equivalent concentrations (BECs) cited in Tables 3 and 4 relate to the "control" values—those measured from a "normal" ICP without these additional ways to attenuate polyatomic ions. The BEC is the solution concentration of analyte that yields a net signal for M^+ of the same magnitude as that for the interfering polyatomic ion. A Sciex ELAN Model 250 with upgraded ion optics is used for the comparative data derived from refs 5 and 9. In general, the ICP operating conditions are selected to yield maximum M^+ signal in each case.

The count rates observed for four of the most troublesome polyatomic ions (ArN^+, ArO^+, ClO^+, and $ArCl^+$) are compared to those seen from our Sciex ELAN instrument in Table 3. For the present work, the total count rates at m/z 54, 56, 51, and 75 are reported and assumed to be due solely to the polyatomic ions. Table 3 shows that the levels of polyatomic ions seen in the present work are indeed much lower than those seen when a comparable nebulizer and desolvator are used on our Sciex ELAN instrument.

BEC values for the two instruments are given in Table 4. The BEC values are particularly useful for comparison because they account for both the background and the analyte signals. In general, the BEC values seen in the present work are superior to those from ref 5. However, the measurements in ref 5 were performed with a home-made ultrasonic nebulizer [28], which was similar in principle but did not yield as intense an aerosol as the commercial nebulizer used in the present work and in ref 9. The BEC values from the present work are comparable to or perhaps somewhat

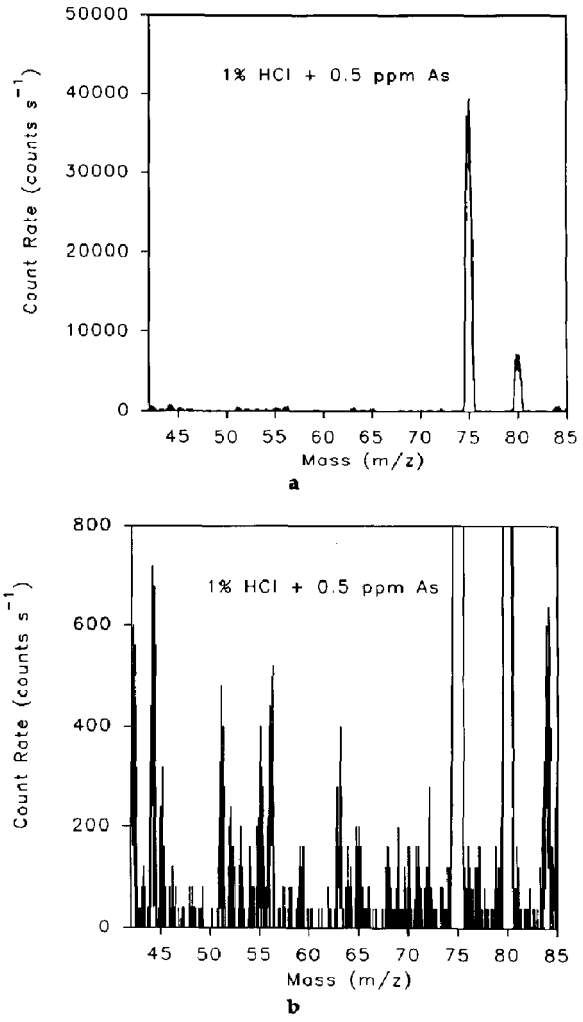

Figure 7. Mass spectrum from 0.5 ppm As in 1% HCl.

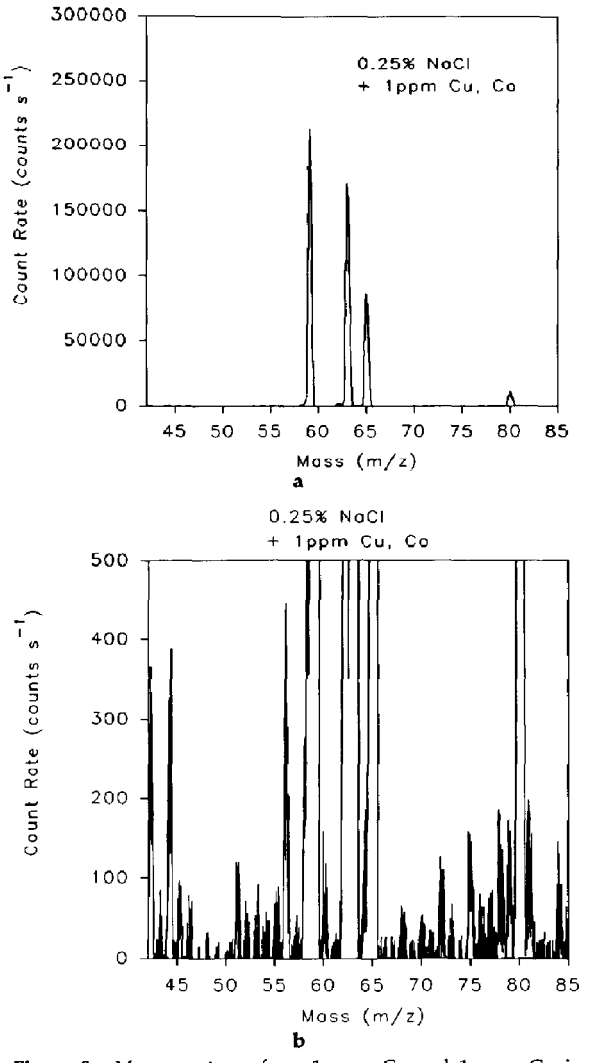

Figure 8. Mass spectrum from 1 ppm Co and 1 ppm Cu in 0.25% NaCl (0.1% Na).

worse than those from the Sciex ELAN instrument used in ref 9. Although the absolute levels of polyatomic ions are quite low for the instrument described in the present work and the companion paper [26], the count rates for analyte ions are also lower than would usually be expected when an ultrasonic nebulizer is employed. The BEC values reported for ref 9 in the far right column of Table 4 are among the best values obtained with commercial instruments. The higher values from ref 5 are more typical.

A detailed comparison of the BEC values in Table 4 with those obtained on commercial instruments with the usual pneumatic nebulizers is even more questionable, so only typical examples are cited. Recent desolvation studies by Lam and McLaren [1], Jakubowski et al. [7, 8], and Tsukahara and Kubota [10] report BEC values for $^{56}Fe^+$ of 74–190 ppb with a spray chamber at 0–30 °C. These BECs improve to 14–55 ppb with a

Table 3. Comparison of count rates for polyatomic ions to the other work with ultrasonic nebulizer with conventional desolvation[a]

		Count rates (counts s^{-1})		
Interferent	Solution	Present work	Ref 5	Ref 9
$^{40}Ar^{14}N^+$	DDW	60	14,100	1,000
$^{40}Ar^{16}O^+$	DDW	200	72,800	12,000
$^{35}Cl^{16}O^+$	1% HCl	400	24,000	50,000
$^{40}Ar^{35}Cl^+$	1% HCl	150	890	1,200

[a]Aqueous samples, heater temperature ~140 °C, condensor temperature ~0 °C.

Table 4. Comparison of BECs to those obtained in other work with ultrasonic nebulizer with conventional desolvation[a]

Analyte	Interferent	BEC (ppb) Present work	Ref 5	Ref 9
$^{54}Fe^+$	$^{40}Ar^{14}N^+$	4	100	0.8
$^{56}Fe^+$	$^{40}Ar^{16}O^+$	0.7	35	0.7
$^{51}V^+$	$^{35}Cl^{16}O^+$[b]	1.8	16	4
$^{76}As^+$	$^{40}Ar^{35}Cl^+$[b]	1.8	1.4	0.3

[a] Aqueous samples, heater temperature ~140 °C, condensor temperature ~0 °C.
[b] Analyte and interferent measured during nebulization of 1% HCl.

desolvation system like that used in the present work. Evans and Ebdon [29] report data that correspond to a BEC of 140 ppb As in 1% HCl with a spray chamber cooled to 5 °C and no additional substances (e.g., N_2, O_2, or organic solvent) added to the plasma. Jarvis et al. [11] list BECs for a VG PQ2 with a cooled spray chamber. These values are cited for Co and are corrected below for isotopic abundance for Fe and for the ionization efficiency of As (estimated to be 30% [11]). With these corrections, the values of Jarvis et al. [11] correspond to BECs of 200 ppb Fe at m/z 54 and 90 ppb Fe at m/z 56 in 1% HNO_3. In 1% HCl, BEC values of 230 ppb V and 120 ppb As are estimated.

Either of these values with pneumatic nebulizers are substantially poorer than our BECs from Table 4. At any rate, the instrument described in the present work yields very low levels of polyatomic ions and BECs that are at least as good as the best values produced by typical commercial instruments based on quadrupoles. Newfangled tricks like adding N_2 or Xe [1, 3–5, 29] or cryogenic desolvation [2, 9] could attenuate some of the interfering ions to still lower levels, if indeed they are due to polyatomic ions and are not simply metal impurities from the solvents. As described in the companion article [26], the background at higher mass-to-charge values (i.e., above ~m/z 80) is also very low (~0.4 counts s^{-1}) for the device described in the present work.

Metal Oxide Ions

Under the conditions that yield maximum M^+ signal, refractory metal oxide ions are fairly abundant, that is, the count rate for MO^+ is 10% of that for M^+ for M = La or U. Moving the sampling position slightly downstream to 15 mm and decreasing the aerosol gas flow rate from 1.30 L min^{-1} to 1.1 L min^{-1} reduces the MO^+/M^+ ratios substantially to the values shown in Table 5. This adjustment of operating conditions induces only a minor sacrifice of 10 to 20% loss of M^+ signal. The values of 0.5% for MoO^+/Mo^+ and ~1% for LaO^+/La^+ and UO^+/U^+ are quite typical of ICP-MS devices with this type of desolvation (i.e., heating at 140 °C followed by cooling at ~0 °C) [1, 7, 9, 10].

Table 5. Sensitivity and MO^+/M^+ ratios for elements that form refractory oxides

Elements	M^+ sensitivity (counts s^{-1} per mg L^{-1})	MO^+/M^+ (%)
$^{98}Mo^+$	180,000	0.5
$^{139}La^+$	3,450,000	1.0
$^{238}U^+$	1,230,000	1.2

The general observation that weakly-bound polyatomic ions like $ArCl^+$ and ArO^+ are at quite low levels while refractory oxide ions like LaO^+ and UO^+ are at usual levels is interesting. Hieftje [30] has suggested that the high degree of spatial selectivity of the lens discriminates against ArO^+, $ArCl^+$, and so on. If these weakly bound ions are not present in the plasma but are created by reactions during the extraction process in the boundary layer inside the edge of the sampler or skimmer, they would not be particularly abundant along the central axis of the beam leaving the skimmer. In contrast, most other ICP-MS devices block photons with a solid baffle along the center line. Such lenses accept only ions that leave the skimmer off center [31]. Perhaps the off-center section of the beam is enriched in polyatomic ions made in the boundary layer; these weakly bound polyatomics are therefore more abundant in spectra from these devices. To test this hypothesis thoroughly, an instrument in which the lens and mass analyzer can be moved radially relative to the skimmer would be required.

Vaughan and Horlick [32] conclude that metal oxide ions are made largely during the extraction process, but their study merely proves that extra metal oxide ions can be seen if the sampling orifice is too small. The authors' view is that refractory metal oxide ions like LaO^+ and UO^+, which have dissociation energies of 8 to 9 eV, are not completely dissociated in the plasma [33–35]. These ions pass through the sampler and skimmer just like the atomic analyte ions and are not rejected preferentially by the lens. Hence, the spatial selectivity of the offset ion lens does not discriminate against MO^+, and the levels of MO^+ seen in the present work are typical of those seen on most ICP-MS devices.

Matrix Interferences

These experiments are performed under conditions that yield maximum Y^+ signal for each lens configuration. The sampling position was 11 mm. Each lens required a slightly different value of aerosol gas flow rate, as shown in Table 1. The measured interference effects are plotted for each analyte and matrix under the three lens configurations (A, B, and C, Figure 1) in Figures 9–11. Again, a highly efficient ultrasonic nebulizer is used in the present work. The high rate of introduction of matrix with this nebulizer would be expected to induce substantial matrix effects [36]. In

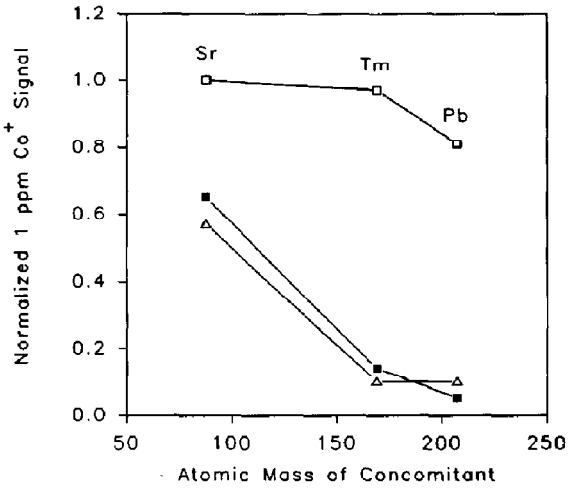

Figure 9. Matrix effect results: normalized Co^+ signal for 1 ppm Co in the presence of Sr, Tm, or Pb, each at 10 mM. (△): lens config. A; (□): lens B; (■): lens C.

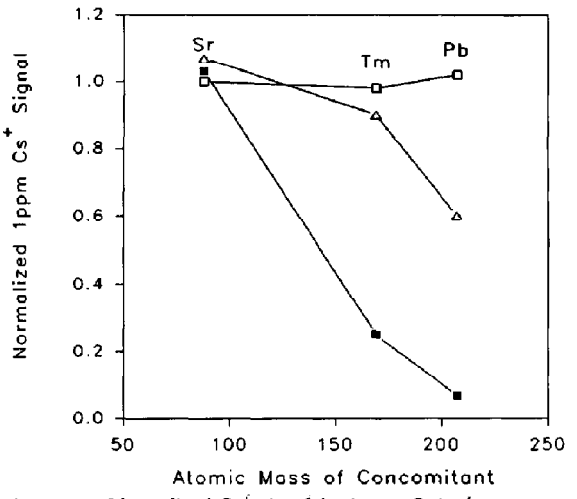

Figure 11. Normalized Cs^+ signal for 1 ppm Cs in the presence of Sr, Tm, or Pb, each at 10 mM. (△): lens config. A; (□): lens B; (■): lens C.

each case, the analyte signal is suppressed severely with lenses A and C, whereas little or no suppression is seen with lens B. For example, Sr and Tm at 10 mM do not cause measurable interference on any of the three analytes with lens B. Lead at 10 mM suppresses Co^+ and Y^+ signal by only 20% (Figures 9 and 10) and causes little interference on the heavier Cs^+ (Figure 11).

Sensitivities and detection limits with the three lenses are given in Table 6. Lens A yields the best sensitivity but is highly vulnerable to matrix effects. Grounding the first cylinder (lens B) involves only a modest sacrifice in sensitivity and detection limits, and matrix effects are minimal. The basic reasons why lenses A and B should result in substantially different matrix effects are not clear at this time. The two configurations differ mainly by only +3 V on the first cylinder (V_1, Figure 1), with only minor differences in the voltages applied to the other electrodes. The extent of matrix effects does not simply increase with the total transmission, because the transmissions of lenses A and B are not that different, and lens C has both poor transmission (i.e., poor sensitivity in Table 6) and bad matrix effects.

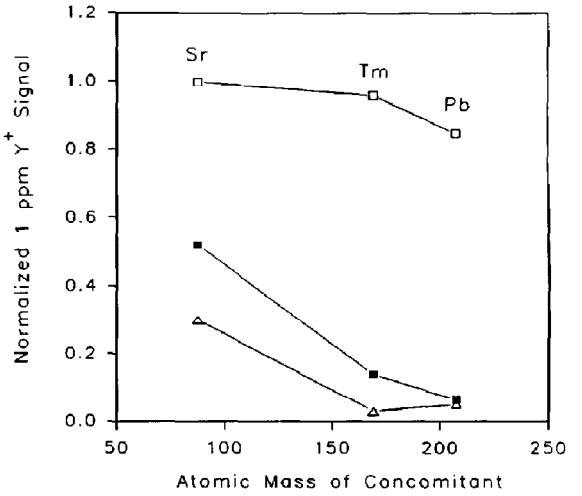

Figure 10. Normalized Y^+ signal for 1 ppm Y in the presence of Sr, Tm, or Pb, each at 10 mM. (△): lens config. A; (□): lens B; (■):lens C.

The matrix concentrations (10 mM) in the present work are the same as those used by Ross and Hieftje [27], who introduced samples with a conventional pneumatic nebulizer. The small matrix effects observed with lens B are comparable to their results with no lens in the second stage, particularly when the higher rate of transport of matrix from the ultrasonic nebulizer used in the present work is considered. The measures taken to reduce matrix effects (i.e., grounding the first lens, rather than removing all the lenses in the second stage) are quite different in our study.

Effect of Matrix on Lens Voltages

At times, we have observed that introduction of a matrix element can affect the apparent voltage applied to the first lens [37]. A similar phenomenon is seen in the present work with lens A. During nebulization of a blank solution, V_1 is set to +3 V and the other lenses are adjusted to maximize signal. When a matrix solution is added, the apparent voltage on lens 1 decreases, as shown in Table 7. If the matrix effect is measured without changing the power supply setting that feeds

Table 6. Analyte sensitivities and detection limits measured with the various lens configurations[a]

Configuration	Sensitivity (counts s^{-1} per mg L^{-1})			Detection limit (ng L^{-1})		
	Co	Y	Cs	Co	Y	Cs
A[b]	1,200,000	1,900,000	3,600,000	2	1	0.5
B	1,000,000	1,200,000	2,500,000	2	2	0.8
C	180,000	480,000	1,000,000	10	4	2

[a] Each configuration was optimized for maximum Y^+ signal using the conditions listed in Table 1 and Table 2.
[b] Ion lens configurations A, B, and C are described in Table 2.

lens 1, analyte signals are suppressed substantially (Figure 12). If the voltage output of the power supply is readjusted to read +3 V with the matrix present, the effect of matrix on analyte signal is not severe, as also shown in Figure 12. The matrix effects on Co^+ and Y^+ signal can also be alleviated in much the same way; data for these elements are not shown. The deviation of apparent voltage on lens 1 is greatest for the heavier matrix element (e.g., for Pb in Table 7), which again agrees roughly with our previous observations [37].

It has been shown both experimentally [23] and by space-charge calculations [23, 24] that adding matrix elements at even modest concentrations can substantially increase the ion current that can be collected leaving the skimmer. If the current drawn by the first lens increases when a matrix element is present, perhaps the power supply that feeds this lens can no longer maintain the prescribed voltage. Thus, the actual voltage applied to the lens drops, unless the nominal voltage output of the power supply is increased to compensate.

Our procedure of readjusting the voltage on lens 1 with the matrix present could prove useful in that it allows use of the more sensitive lens A configuration with minimal matrix effects. Caruso and co-workers [38, 39] have reported at length on a successful tactic for mitigating matrix effects, which they call matrix tuning. The ion lens voltages are adjusted to maximize analyte signal with the matrix actually present. This adjustment of lens voltages is sometimes done during nebulization of the actual sample of interest, rather than a standard. This procedure differs in detail from our method of resetting the voltage applied to lens 1 to its original value with the matrix present. Nevertheless, both approaches mitigate matrix effects significantly, perhaps for similar basic reasons. All these instrumental modifications for attenuating matrix effects require much more fundamental and applied study before they are understood properly.

Table 7. Influence of matrix element on apparent voltage applied to lens 1

Matrix	Apparent voltage on lens 1[a] (V)
None	+3.0
Sr[b]	+2.5
Tm	2.0
Pb	1.0

[a] Measured from output meter on power supply to lens 1.
[b] Matrix elements present at 10 mM.

Conclusion

This article and its companion [26] describe a quadrupole ICP-MS device with the following attributes: low levels of polyatomic ions, minimal matrix interferences, low background, and high tolerance to plugging from deposited solids. The analyte sensitivity is about 10 times lower than that expected from common commercial instruments with an ultrasonic nebulizer. Experiments to test these performance figures for the analysis of difficult samples with this ICP-MS device are under way in our laboratory.

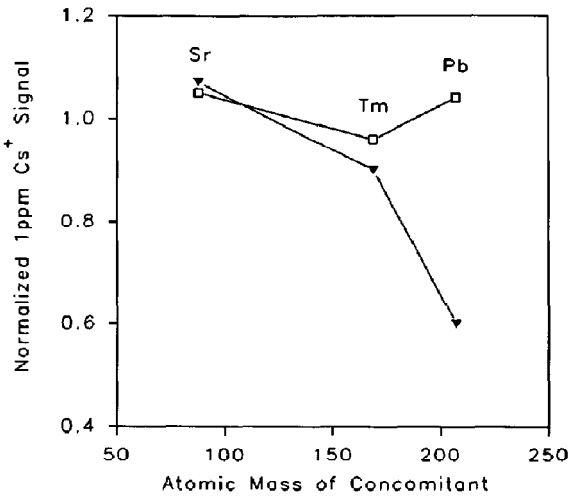

Figure 12. Normalized Cs^+ signal for 1 ppm Cs in the presence of Sr, Tm, or Pb, each at 10 mM. (▼): lens 1 power supply not adjusted when matrix present; (□): lens 1 power supply readjusted to +3.0 V output when matrix present. See text for explanation.

Acknowledgments

The Ames Laboratory is operated by Iowa State University for the U.S. Department of Energy under contract no. W-7405-Eng-82. This research was supported by the Office of Basic Energy Sciences, Division of Chemical Sciences. Financial support from the U.S. Department of Commerce through the Center for Advanced Technology Development for construction of the ICP-MS device is also gratefully acknowledged. The ultrasonic nebulizer was provided by Cetac Technologies, Inc., Omaha, Nebraska.

References

1. Lam, J. W.; McLaren, J. W. *J. Anal. Atom. Spectrom.* **1990**, *5*, 419–445.
2. McLaren, J. W.; Lam, J. W.; Gustavsson, A. *Spectrochim. Acta B* **1990**, *45*, 1091–1094.
3. Lam, J. W.; Horlick, G. *Spectrochim. Acta B* **1990**, *45*, 1313–1325.
4. Ebdon, L.; Evans, E. H.; Barnett, N. W. *J. Anal. Atom. Spectrom.* **1989**, *4*, 505–508.
5. Smith, F. G.; Wiederin, D. R.; Houk, R. S. *Anal. Chem.* **1991**, *63*, 1458–1462.
6. Houk, R. S.; Fassel, V. A.; Flesch, G. D.; Svec, H. J.; Gray, A. L.; Taylor, C. E. *Anal. Chem.* **1980**, *52*, 2283–2289.
7. Jakubowski, N.; Feldman, I.; Stuewer, D. *Spectrochim. Acta B* **1992**, *47*, 107–118.
8. Jakubowski, N.; Feldman, I.; Stuewer, D.; Berndt, H. *Spectrochim. Acta B* **1992**, *47*, 119–129.
9. Alves, L. C.; Wiederin, D. R.; Houk, R. S. *Anal. Chem.* **1992**, *64*, 1164–1169.
10. Tsukahara, R.; Kubota, M. *Spectrochim. Acta B* **1990**, *45*, 581–589.
11. Jarvis, K. E.; Gray, A. L.; Houk, R. S. *Handbook of Inductively Coupled Plasma Mass Spectrometry*; Blackie: Glasgow, 1991.
12. Hutton, R. C. U. S. Patent 4760253, 1988.
13. Bradshaw, N.; Hall, E. F. H.; Sanderson, N. E. J. *Anal. Atom. Spectrom.* **1989**, *4*, 801–803.
14. Morita, M.; Ito, H.; Uehiro, T.; Otsuka, K. *Anal. Sci.* (Japan) **1989**, *5*, 609–610.
15. Rowan, J. T.; Houk, R. S. *Appl. Spectrosc.* **1989**, *43*, 976–980.
16. King, F. L.; Harrison, W. W. *Int. J. Mass Spectrom. Ion Proc.* **1989**, *89*, 171–185.
17. Duckworth, D. C.; Marcus, R. K. *Appl. Spectrosc.* **1990**, *44*, 649–655.
18. Olivares, J. A.; Houk, R. S. *Anal. Chem.* **1986**, *58*, 20–25.
19. Tan, S. H.; Horlick, G. *J. Anal. Atom. Spectrom.* **1987**, *2*, 745–763.
20. Gregoire, D. C. *Appl. Spectrosc.* **1987**, *41*, 897–903; *Spectrochim. Acta B* **1987**, *42*, 895–907.
21. Kawaguchi, H.; Tanaka, T.; Nakamura, T.; Morishita, M.; Mizuike, A. *Anal. Sci.* (Japan) **1987**, *3*, 305–308.
22. Beauchemin, D.; McLaren, J. W.; Berman, S. S. *Spectrochim. Acta B* **1987**, *42*, 467–490.
23. Gillson, G. R.; Douglas, D. J.; Fulford, J. E.; Halligan, K. W.; Tanner, S. D. *Anal. Chem.* **1988**, *60*, 1472–1474.
24. Tanner, S. D. *Spectrochim. Acta B* **1992**, *47*, 809–823.
25. Thompson, J. J.; Houk, R. S. *Appl. Spectrosc.* **1987**, *41*, 801–806.
26. Hu, K.; Clemons, P. S.; Houk, R. S. *J. Am. Soc. Mass Spectrom.* **1993**, *4*.
27. Ross, B. C.; Hieftje, G. M. *Spectrochim. Acta B* **1991**, *46*, 955–962.
28. Bear, B. R.; Fassel, V. A. *Spectrochim. Acta B* **1986**, *41*, 1089–1113.
29. Evans, E. H.; Ebdon, L. *J. Anal. Atom. Spectrom.* **1989**, *4*, 299–300.
30. Hieftje, G. M. *Winter Conference on Plasma Spectrochemistry*; San Diego, CA, January, 1992; paper PL-6.
31. Vaughan, M. A.; Horlick, G. *Spectrochim. Acta B* **1990**, *45*, 1301–1311.
32. Vaughan, M. A.; Horlick, G. *Spectrochim. Acta B* **1990**, *45*, 1289–1299.
33. Douglas, D. J. In *ICPs in Analytical Atomic Spectrometry*, 2nd ed.; Montaser, A. and Golightly, D., Eds.; VCH: New York, 1992.
34. Longerich, H. P. *J. Anal. Atom. Spectrom.* **1989**, *4*, 491–497.
35. Kubota, M.; Fudagawa, N.; Kawase, A. *Anal. Sci.* (Japan) **1989**, *5*, 701–706.
36. Tarr, M. A.; Zhu, G.; Browner, R. F. *Appl. Spectrosc.* **1991**, *45*, 1424–1432.
37. Crain, J. S.; Houk, R. S.; Smith, F. G. *Spectrochim. Acta B* **1988**, *43*, 1355–1364.
38. Wang, J.; Shen, W. L.; Sheppard, B. S.; Evans, E. H.; Fricke, F. L.; Caruso, J. A. *J. Anal. Atom. Spectrom.* **1990**, *5*, 445–449.
39. Sheppard, B. S.; Shen, W. L.; Caruso, J. A. *Am. Soc. Mass Spectrom.* **1991**, *2*, 355–361.